

# Free Boundary, High Beta Equilibrium in a Large Aspect Ratio Tokamak with Nearly Circular Plasma Boundary

H. Qin      A. Reiman

September 25, 1996

## Abstract

An analytic solution is obtained for free-boundary, high-beta equilibria in large aspect ratio tokamaks with a nearly circular plasma boundary. In the absence of surface currents at the plasma-vacuum interface, the free-boundary equilibrium solution introduces constraints arising from the need to couple to an external vacuum field which is physically realizable with a reasonable set of external field coils. This places a strong constraint on the pressure profiles that are consistent with a given boundary shape at high  $\epsilon\beta_p$ . The equilibrium solution also provides information on the flux surface topology. The plasma is bounded by a separatrix. Increasing the plasma pressure at fixed total current causes the plasma aperture to decrease in a manner that is described.

PACS: 52.30.Bt, 52.55.Fa, 52.55.-s, 52.65.Kj

**MASTER**

## 1 Introduction

It is desirable to achieve high  $\beta$  in tokamaks for the purpose of developing an economic fusion reactor. It has long been recognized that there is an equilibrium constraint on high  $\beta$  tokamaks arising from the appearance of a separatrix which moves into the plasma. This effect has been observed in TFTR.[1, 2] When  $\epsilon\beta_p$  is raised to a sufficiently high value, the plasma aperture becomes constricted by a naturally arising inboard poloidal field null which prevents further increase of the plasma pressure. This is easily understood in terms of a simple physical model. As the plasma pressure is increased, the externally applied vertical field is increased to maintain

## **DISCLAIMER**

This report was prepared as an account of work sponsored by an agency of the United States Government. Neither the United States Government nor any agency thereof, nor any of their employees, make any warranty, express or implied, or assumes any legal liability or responsibility for the accuracy, completeness, or usefulness of any information, apparatus, product, or process disclosed, or represents that its use would not infringe privately owned rights. Reference herein to any specific commercial product, process, or service by trade name, trademark, manufacturer, or otherwise does not necessarily constitute or imply its endorsement, recommendation, or favoring by the United States Government or any agency thereof. The views and opinions of authors expressed herein do not necessarily state or reflect those of the United States Government or any agency thereof.

## **DISCLAIMER**

**Portions of this document may be illegible in electronic image products. Images are produced from the best available original document.**

equilibrium. On the inboard side of the tokamak, the applied vertical field opposes the poloidal field produced by the plasma current. A null point is produced, which moves into the plasma as the the vertical field is increased for a fixed plasma current. This simple model, while explaining the main features of the experimentally observed effect, does not take into account the effects of changing current and pressure profiles, or the application of multipolar external fields. In particular, it has been suggested that the equilibrium  $\beta$  limit can be circumvented by a sequence of "flux-conserving equilibria" which maintain the  $q$  profile. We address these issues in this paper in the context of an analytic solution for free-boundary, high-beta equilibria in large aspect ratio tokamaks with a nearly circular plasma boundary.

Cowley *et al*[3] have obtained a fixed boundary tokamak equilibrium solution valid for large aspect ratio and very high  $\beta$ . In this paper, we extend that solution to include the matching to an externally imposed vacuum field, under the added assumption that the shape of the plasma boundary is nearly circular. For a fixed boundary solution it is possible to arbitrarily and independently specify the shape of the plasma boundary, as well as the pressure and  $q$  profiles in the plasma (where  $q$  is the "safety factor"). The free-boundary equilibrium introduces constraints arising from the need to couple to an external vacuum field which is physically realizable with a reasonable set of external field coils. We will see that this places a strong constraint on the profiles that are consistent with a given boundary shape at high  $\epsilon\beta_p$ .

In Section 2 we obtain the solution to the Grad-Shafranov equation in the plasma interior, assuming  $\epsilon \ll \beta \leq 1$  (where  $\epsilon$  is the inverse aspect ratio). This is a generalization of the treatment of Cowley *et al*, who assume  $\beta = O(1)$ .

In Section 3 we match to the solution in the vacuum region under the assumption that the plasma boundary is circular, and we describe the topology of the solution. We take the field to be continuous across the plasma-vacuum interface. In taking the component of the magnetic field parallel to the boundary to be continuous, we are assuming that there is no surface current.

In Section 4 we perturb about the solution obtained in the previous section to investigate the effect of a small modification in the shape of the plasma boundary.

Finally, in Section 5 we discuss our solutions and present some conclusions.

## 2 Solution of Grad-Shafranov equation in the Plasma Interior for $\epsilon \ll \beta \leq 1$

In this section we obtain the solution to the Grad-Shafranov equation in the plasma interior, assuming  $\epsilon \ll \beta \leq 1$ . We generalize the treatment of Cowley *et al*, who assume  $\beta = O(1)$ . We take  $\beta = O(\epsilon^\gamma)$  ( $0 \leq \gamma < 1$ ). This is to be compared with the conventional low  $\beta$  tokamak ordering,  $\beta = O(\epsilon^2)$ , and the conventional high  $\beta$  tokamak ordering,  $\beta = O(\epsilon)$ [4]. For  $\gamma < 1$  a boundary layer appears in the solution of the Grad-Shafranov equation, with the width of the boundary layer depending on the value of  $\gamma$ .

It is convenient to introduce the following normalization[3]:

$$\bar{x} = x/a, \bar{z} = z/a, \bar{R} = R_0(1 + \epsilon\bar{x}), \epsilon = a/R_0, \bar{\psi} = \psi/\psi_{max}. \quad (1)$$

$$\bar{F} = \frac{a^2}{R_0\psi_{max}} F \sim 1, \bar{p} = \frac{\mu_0 a^4}{\psi_{max}^2} p \sim \epsilon^\gamma (0 \leq \gamma < 1). \quad (2)$$

Here  $\psi_{max}$  is  $\psi$  at the plasma boundary, corresponding to  $p(\psi_{max}) = 0$ , and  $a$  is the scale length of the plasma in a poloidal cross-section. In the circular boundary case,  $a$  is the minor radius. By choosing  $\bar{F} = O(1)$  and  $\bar{p} = O(\epsilon^\gamma)$  ( $0 \leq \gamma < 1$ ), we imply that  $q = O(1)$  and  $\beta = O(\epsilon^2 \bar{\beta}_p) = O(\epsilon^\gamma)$  ( $0 \leq \gamma < 1$ ), where  $\bar{\beta}_p \equiv (a^2 R_0^2 / \psi_{max}^2) \mu_0 p_{max}$ , and  $\gamma$  is chosen such that  $\epsilon^\gamma = \epsilon^2 \bar{\beta}_p$ . In the normalized variables, we get the dimensionless Grad-Shafranov equation:

$$\epsilon^2 [(1 + \epsilon\bar{x}) \frac{\partial}{\partial \bar{x}} \frac{1}{1 + \epsilon\bar{x}} \frac{\partial}{\partial \bar{x}} + \frac{\partial^2}{\partial \bar{z}^2}] \bar{\psi} = (1 + \epsilon\bar{x})^2 \frac{d\bar{p}}{d\bar{\psi}} + \bar{F} \frac{d\bar{F}}{d\bar{\psi}}. \quad (3)$$

The perturbative solution of this equation with respect to small  $\epsilon$  is singular. It is a boundary layer problem. Physically, the leading order force balance is between plasma pressure and toroidal field which does not involve the differential operator. Compared with the conventional low  $\beta$  and high  $\beta$  ordering, this ordering actually simplifies the problem. From now on, we will drop the bars on the normalized variables except where explicitly stated. Let:

$$\gamma = m/n, \alpha = \epsilon^{1/n}. \quad (4)$$

Where  $m, n$  are integers and  $m < n$ . When  $\gamma = 0$ , we choose  $m = 0, n = 1$ .

Expanding  $\psi$  and  $FF' \equiv G$  in the small parameter  $\alpha = \epsilon^{1/n}$ , we have:

$$\psi = \psi_0 + \alpha^1 \psi_1 + \alpha^2 \psi_2 + \dots, \quad (5)$$

$$FF' \equiv G = G_0 + \alpha^1 G_1 + \alpha^2 G_2 + \dots. \quad (6)$$

After expanding the Grad-Shafranov equation (see Appendix A for details), we obtain the equation determining the core solution:

$$2xp'(\psi_0) + G_{m+n}(\psi_0) = 0. \quad (7)$$

For given  $p$  and  $G$  profiles, this equation determines  $x(\psi_0)$ . In the form of unnormalized variables, (7) is:

$$2\mu_0 R_0^2 xp'(\psi_0) + aG_{m+n}(\psi_0) = 0. \quad (8)$$

The domain of validity of the core solution extends to the plasma boundary on the inboard side of the mid-plane. If we let  $a$  correspond to the  $x$  coordinate of the inboard intersection of the plasma boundary with the mid-plane, we get the relation

$$-2\mu_0 R_0^2 p'(\psi_{max}) + G_{m+n}(\psi_{max}) = 0. \quad (9)$$

The value of  $q$  on each flux surface is dominated by the contribution from the core, so that[3]

$$q(\psi_0) = \frac{\pm F_0(\psi_0) \sqrt{1-x^2}}{\pi \frac{d\psi_0}{dx}}. \quad (10)$$

When  $\gamma > 0$ ,  $F_0' = 0$ , so  $F_0$  is a constant. In this case, integration of equation (10) yields  $F_0 = 2\Psi_t$ , where  $\Psi_t$  is the total toroidal flux.

For the boundary layer, the differential equation for  $\psi_0$  is:

$$-[1 + (\frac{r_b'(\theta)}{r_b(\theta)})^2] \frac{\partial^2 \psi_0}{\partial t^2} = 2r_b(\theta) \cos \theta \frac{dp}{d\psi_0} + G_{m+n}(\psi_0), \quad (11)$$

where

$$r = r_b(\theta) - \epsilon^\lambda t, \quad (12)$$

and  $r_b(\theta)$  is the radial coordinate of the plasma-vacuum boundary. The quantity  $\epsilon^\lambda$  is the width of the boundary layer, where  $\lambda$  is defined to be  $\lambda \equiv (1 - \gamma)/2$ .

To 0th and 1st order in  $\delta$  the coefficient  $[1 + (\frac{r_b'(\theta)}{r_b(\theta)})^2]$  can be dropped, where  $\delta$  is the small parameter measuring the deviation of the boundary from circularity. Substituting  $G_{m+n}(\psi_0)$  from equation (7), we obtain

$$-\frac{\partial^2 \psi_0}{\partial t^2} = 2[x_{core}(\psi_0) - \cos \theta r_b(\theta)] \frac{dp}{d\psi_0}. \quad (13)$$

Multiplying equation (13) by  $\partial\psi_0/\partial t$ , integrating from  $t = \infty$  and choosing  $\partial\psi_0/\partial t \rightarrow 0$  as  $\psi \rightarrow \psi_{core}$ , we get

$$\left(\frac{\partial\psi_0}{\partial t}\right)^2 = 4 \int_{\psi_{core0}(\cos\theta r_b(\theta))}^{\psi_0} d\psi' [x(\psi') - \cos\theta r_b(\theta)] \frac{dp}{d\psi'} \quad (14)$$

$$= 4p[x(\psi') - \cos\theta r_b(\theta)]|_{\psi_{core0}(\cos\theta r_b(\theta))}^{\psi_0} - 4 \int_{\cos\theta r_b(\theta)}^{x(\psi_0)} p(\psi_0(x)) dx, \quad (15)$$

where  $\psi_0(x)$  is the core solution for  $\psi_0$  as a function of  $x$ . To obtain this expression, we have integrated by parts. Assuming that  $p = 0$  on the plasma boundary, the radial derivative of  $\psi_0$  there is given by

$$\left(\frac{\partial\psi_0}{\partial r}\right)^2|_{\psi_0=1} = 4\epsilon\bar{\beta}_p \int_{x(1)}^{\cos\theta r_b(\theta)} p(\psi_0(x)) dx. \quad (16)$$

The  $\epsilon\bar{\beta}_p$  scaling reflects the fact that the width of the boundary layer scales like  $(\epsilon\bar{\beta}_p)^{-1/2}$ .

The thickness of the boundary layer goes to zero at  $\theta = \pi$ . The boundary layer may terminate at a smaller value of  $\theta$ . In that case, a segment of the plasma boundary is described by the core solution, and must be a straight line. If the boundary layer extends all the way to  $\theta = \pi$ , then it follows from equation (16) that

$$\left(\frac{\partial\psi_0}{\partial r}\right)^2|_{\psi_0=1, \theta=\pi} = 0. \quad (17)$$

The leftmost boundary on the mid-plane is then a zero point of the poloidal field.

### 3 Free-Boundary Solution with Circular Boundary

In this section we will match the equilibrium solution in the plasma interior to the solution in the vacuum region under the assumption that the plasma boundary is circular. We adopt boundary conditions at infinity appropriate for the situation where we have a set of equilibrium coils located far from the plasma. The matching at the plasma-vacuum boundary will impose a strong constraint, uniquely determining the value of the quantity  $p(\psi_0(x))$  in the plasma interior. We will also look at the topology of the magnetic field, and will find that the plasma-vacuum boundary coincides with a separatrix.

To the lowest order in  $\epsilon$ , the vacuum flux  $\psi_v$  satisfies Laplace equation:

$$\nabla^2\psi_v = 0, \quad (18)$$

whose general solution is:

$$\psi_v = a_0 + b_0 \ln r + \sum_{n=1}^{\infty} (a_n r^n + b_n r^{-n}) \cos n\theta. \quad (19)$$

We take the plasma-vacuum boundary to be a circle. The radius of the circle,  $a$  must be consistent with Eq. (9). In normalized form, the equation for the boundary is:

$$r_b(\theta) = 1. \quad (20)$$

Due to the continuity of the normal component of the magnetic field,  $\psi$  must be continuous across the plasma-vacuum interface:

$$\psi_v|_{r_b(\theta)} = \psi_0|_{r_b(\theta)} = 1. \quad (21)$$

Therefore,

$$a_0 = 1, a_n = -b_n (n > 0) \quad (22)$$

There are two pieces to the magnetic field solution in the vacuum region. One piece decays radially outward as we move away from the plasma, and it corresponds to the field produced by the plasma currents. The second piece increases as we move away from the plasma boundary into the vacuum region. This part of the field is produced by the currents in the external field coils.

The quantity  $b_0$  is related to the total current through the plasma. From  $B_p = \frac{\nabla\psi}{R} \times \hat{\phi}$  and  $\mu_0 I_t = \oint B_p dl$ , we get:

$$I_t = \frac{2\pi\psi_{max}}{\mu_0 R_0} b_0. \quad (23)$$

We regard the external equilibrium coils as being far from our large aspect ratio tokamak plasma. Far from the plasma, the  $\theta$  dependent part of the field that is driven by the plasma currents decays like  $r^{-n}$ , and is small compared to the  $\theta$  dependent part of the field that is driven by the external coils. The field produced by the coils at large  $r$  determines the  $a_n$  for  $n > 0$ . On a circular reference surface at  $r = r_l$ ,  $r_l \gg a$ , we have

$$a_n = \frac{1}{r_l^n \pi} \int_0^{2\pi} \psi_v(r = r_l, \theta) \cos n\theta d\theta. \quad (24)$$

The  $\theta$  independent part of the field far from the plasma is determined by  $b_0$ :

$$b_0 = \frac{1}{\ln r_l 2\pi} \int_0^{2\pi} \psi_v(r = r_l, \theta) d\theta - 1. \quad (25)$$



This part of the field is determined by the total plasma current, and is independent of the external coils.

If we make no further assumptions, there will in general be a discontinuity in the radial derivative of  $\psi$  at the plasma vacuum interface. This would correspond to a surface current. If the equilibrium is rapidly changing, for example if the plasma  $\beta$  is being rapidly ramped up, then we have no reason to rule out the existence of a localized edge current, and the equations tell us that in general such a current will exist. On the other hand, a strongly localized current is dissipated quite rapidly by any finite resistivity. If we are interested in the equilibrium solution on a somewhat longer time scale, it is reasonable to make the assumption that there is no surface current. That is what we will assume. The zero surface-current assumption implies the continuity of the parallel component of the magnetic field plasma-vacuum boundary, giving:

$$\left(\frac{\partial\psi_v}{\partial r}\Big|_{\psi_v=1}\right)^2 = \left(\frac{\partial\psi_0}{\partial r}\Big|_{\psi_0=1}\right)^2. \quad (26)$$

The boundary layer extends to  $\theta = \pi$ . (If it did not, that would imply that a segment of the plasma boundary would be a straight line, which contradicts the assumption that the boundary is circular.) At  $\theta = \pi$  we get

$$\left(\frac{\partial\psi_v}{\partial r}\Big|_{\psi_v=1}\right)^2 = 0. \quad (27)$$

This gives an equilibrium constraint that must be satisfied between the externally imposed equilibrium field and the plasma current:

$$b_0 + \sum_{n=1}^{\infty} a_n n (-1)^n = 0. \quad (28)$$

The continuity of the parallel component of the magnetic field, along with equations (20) and (16), give us an equilibrium constraint that must be satisfied everywhere along the plasma-vacuum interface:

$$\left(\frac{\partial\psi_v}{\partial r}\Big|_{\psi_v=1}\right)^2 = 4\epsilon\bar{\beta}_p \int_{-1}^{\cos\theta} p(x) dx, \quad (29)$$

where we have written  $p(x) \equiv p(\psi_0(x))$ . Differentiating, we obtain an expression for  $p$ :

$$p(\cos\theta) = \frac{1}{2\epsilon\bar{\beta}_p} \left(\frac{\partial\psi_v}{\partial r}\Big|_{\psi_v=1}\right) \frac{d}{d\cos\theta} \left(\frac{\partial\psi_v}{\partial r}\Big|_{\psi_v=1}\right).$$

This gives

$$p(\psi_0(x)) = \frac{1}{2\epsilon\bar{\beta}_p} \left[ b_0 + \sum_{n=1}^{\infty} a_n n T_n(x) \right] \sum_{n=1}^{\infty} a_n n T'_n(x), \quad (30)$$

where the  $T_n(x)$  ( $n = 1, 2, \dots$ ) are Chebyshev polynomials.

For a given externally applied equilibrium field, and a given total plasma current, Eq. (30) determines the pressure as a function of  $x$  in the plasma core. We still have the freedom to specify one additional profile in the interior (e.g. the current profile) to uniquely determine the interior solution. Alternatively, if we are given the solution in the plasma interior,  $p(x)$  is specified, and we can take the square root of Eq. (29) to construct the unique external field required to maintain the equilibrium with a circular boundary.

In practice, only a few low  $n$  values of the  $a_n$  will be non-negligible. The higher  $n$  Fourier components of the vacuum field decay rapidly away from the external field coils. Retaining only the first few terms on the right hand side of Eq. (30), we find that only a restricted set of  $p(x)$  profiles can be reasonably supported with a circular boundary. This is to be contrasted with the fixed boundary solution, where the pressure and current profiles could be arbitrarily specified.

Let's look at the special case where the external field is uniform and vertical at infinity. Now the boundary condition for  $\psi_v$  at a large radius  $r_l$  is

$$B = \frac{\nabla\psi}{R} \times \hat{\phi} \rightarrow B_v \hat{z}. \quad (31)$$

In this case, it is easy to get

$$\psi_v = 1 + b_0 \ln r + a_1(r - 1/r) \cos \theta, \quad (32)$$

and the constraint on the coefficients

$$b_0 = 2a_1, \quad (33)$$

which is the special form of equation (28). The special form here for equation (30) is

$$p(\psi_0(x)) = \frac{1}{2\epsilon\beta_p} b_0^2 (1 + x). \quad (34)$$

The quantity  $a_1$  is related to the vertical field at infinity,

$$B_v = \frac{\psi_{max}}{R_0 a} a_1. \quad (35)$$

Equation (33) is the hoop force balance in the high  $\beta$  case,

$$I_t \mu_0 = 4\pi a B_v. \quad (36)$$

With equation (34) we get an expression for the required vertical field as a function of the pressure. Expressing the result in unnormalized variables, and using

$$p\left(\frac{x}{a}\right) = \frac{p_{max}\left(1 + \frac{x}{a}\right)}{2}, \quad (37)$$

we get

$$B_v = \frac{\mu_0 \epsilon^{5/2} R_0^2 p_{max}}{2\psi_{max}}. \quad (38)$$

This is to be compared with the low- $\beta$  result (see, for example, [4]) where besides pressure several other terms come into the expression for  $B_v$ . However, it is already the case in the conventional high- $\beta$  ordering that the pressure dependence dominates the other terms.[4]

An important figure of merit for tokamak equilibria is

$$\beta_I \equiv \frac{4 \int p \, dV}{R_0 \mu_0 I_t^2}. \quad (39)$$

This measures the plasma pressure that is supported for a given plasma current. In our solution  $\beta_I$  can be obtained explicitly from equation (34),

$$\int_{-1}^1 p(x) 2(1-x^2)^{1/2} dx = \frac{b_0^2 \pi}{2\epsilon \beta_p}. \quad (40)$$

In unnormalized form, we have

$$\begin{aligned} \int p \, dV &= 2\pi R_0 \int_{-a}^a p(x) 2(a^2 - x^2)^{1/2} dx \\ &= 2\pi R_0 \frac{b_0^2 \pi}{2\epsilon \beta_p} a^2 \frac{\psi_{max}^2}{\mu_0 a^4} = \frac{\epsilon^{-2} \mu_0 I_t^2 R_0}{4\epsilon \beta_p}. \end{aligned} \quad (41)$$

Thus,

$$\beta_I \bar{\beta}_p = \epsilon^{-3}. \quad (42)$$

This relation is a consequence of our assumption that there is no surface current at the plasma-vacuum interface.

Now we turn to the topological structure of the vacuum field associated with a circular plasma boundary. On the plasma-vacuum boundary, the poloidal field vanishes at  $\theta = \pi$  and is finite elsewhere. It is straightforward

to verify that at the point ( $r = 1, \theta = \pi$ ), the first and the second derivatives are all zero. The third derivatives at this point are as follows:

$$\frac{\partial^3 \psi_v}{\partial r^3} = \frac{2b_0}{r^3} + \sum_{n=1}^{\infty} a_n n [(n-1)(n-2)r^{n-3} + (n+1)(n+2)r^{-n-3}] T_n(y), \quad (43)$$

$$\frac{\partial^3 \psi_v}{\partial r^3} \Big|_{r=1, \theta=\pi} = \sum_{n=1}^{\infty} 2n^3 a_n (-1)^n, \quad (44)$$

$$\frac{\partial^3 \psi_v}{\partial r^2 \partial \theta} \Big|_{r=1, \theta=\pi} = 0, \quad (45)$$

$$\frac{\partial^3 \psi_v}{\partial r \partial \theta^2} = \sum_{n=1}^{\infty} a_n n (r^{n-1} + r^{-n-1}) [T_n''(y)(1-y^2) - T_n'(y)y], \quad (46)$$

$$\frac{\partial^3 \psi_v}{\partial r \partial \theta^2} \Big|_{r=1, \theta=\pi} = \sum_{n=1}^{\infty} 2a_n n T_n'(-1) = -\frac{\partial^3 \psi_v}{\partial r^3} \Big|_{r=1, \theta=\pi}, \quad (47)$$

$$\frac{\partial^3 \psi_v}{\partial \theta^3} \Big|_{r=1, \theta=\pi} = 0. \quad (48)$$

The identity  $T_n'(-1) = (-1)^{n+1} n^2$  has been used. The Taylor's expansion at ( $r = 1, \theta = \pi$ ) is :

$$\psi_v = 1 + \frac{\partial^3 \psi_v}{\partial r^3} \Big|_{r=1, \theta=\pi} \frac{(r-1)^3}{3!} + 3 \frac{\partial^3 \psi_v}{\partial r \partial \theta^2} \Big|_{r=1, \theta=\pi} \frac{(r-1)(\theta-\pi)^2}{3!}. \quad (49)$$

The equations for the level lines passing through this point can be obtained by setting  $\psi_v = 1$ ,

$$(r-1)^3 - 3(r-1)(\theta-\pi)^2 = 0. \quad (50)$$

Thus there are three such lines:

$$r-1 = \pm \sqrt{3}(\theta-\pi), r=1. \quad (51)$$

Since the vacuum solution is valid onto the surface  $r(\theta) = 1$ , which is itself a flux surface, we conclude that the topological structure of the flux surfaces near the point ( $r = 1, \theta = \pi$ ) is "K-shaped". More precisely, we can verify that at this point all the three angles between these three lines are equal (see figure 1),

$$\angle A_1 = \angle A_2 = \angle A_3 = \pi/3. \quad (52)$$

Figure 1 is the contour plot for the  $\psi_v$  described by equation (32), where the vacuum field is uniform and vertical at infinity.

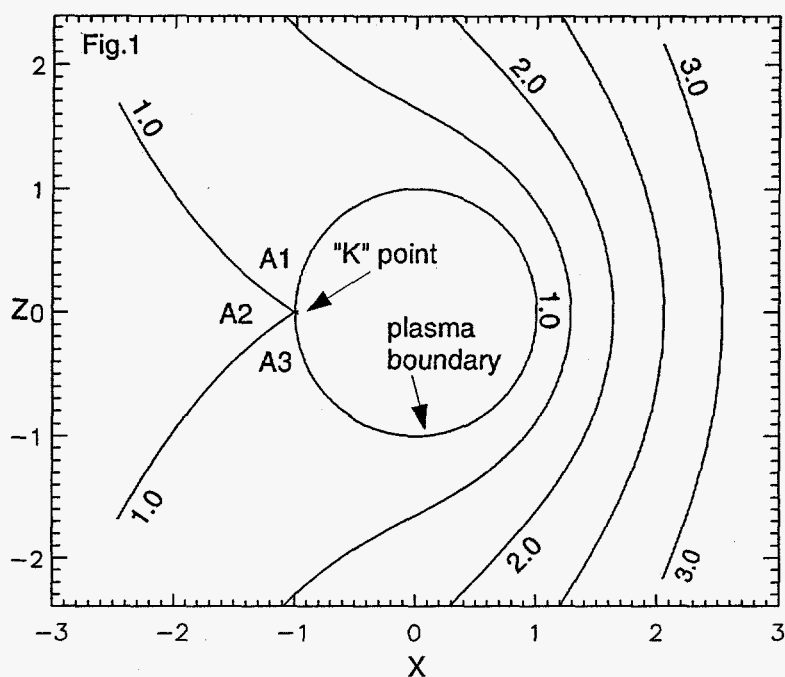


Figure 1: Contour plot for vacuum solution with circular boundary

## 4 Free-Boundary Solution with Perturbed Circular Boundary

In this section we perturb about the solution obtained in the previous section to investigate the effect of a small modification in the shape of the plasma boundary. We use a parameter  $\delta \ll 1$  to measure the deviation of the boundary from circularity,  $r_{b1}(\theta) \equiv [r_b(\theta) - 1] = O(\delta)$ . The corresponding perturbations in  $G_{m+n}$  and  $p$  from those which give a circular boundary are also of order  $\delta$ . Our approach is to specify the perturbed plasma boundary  $r_{b1}(\theta)$  and solve for the perturbed pressure profile  $p_1(x) \equiv p_1(\psi_0(x))$ .

Let

$$p(x) = p_0(x) + p_1(x), \quad (53)$$

$$r_b(\theta) = 1 + r_{b1}(\theta), \quad (54)$$

$$a_n = a_n^{(0)} + a_n^{(1)}, b_n = b_n^{(0)} + b_n^{(1)}, \quad (55)$$

$$\psi_0 = \psi_0^{(0)} + \psi_0^{(1)}, \quad (56)$$

$$\psi_v = \psi_v^{(0)} + \psi_v^{(1)}. \quad (57)$$

As before, the  $a_n, b_n$  are the coefficients in the series solution of  $\psi_v$  which satisfies the Laplace equation. The  $a_n^{(0)}, b_n^{(0)}$  are the unperturbed coefficients, and  $a_n^{(1)}, b_n^{(1)}$  are the first order coefficients with respect to the small distortion from a circular boundary. Also,  $r_{b1}$  is the first order plasma boundary, and  $\psi_0^{(1)}$  and  $\psi_v^{(1)}$  are the first order core and vacuum solution. We expand about a conveniently chosen circular boundary equilibrium solution. We can arbitrarily specify the major and minor radii of the circular boundary solution. We choose them so that the circular boundary coincides with the perturbed plasma boundary at the two points where it crosses the mid-plane. The perturbed plasma boundary then goes through  $x = \pm 1$ , that is:

$$r_{b1}(\pm\pi) = 0. \quad (58)$$

This simplifies the calculation, because  $p(x)$  and  $p_0(x)$  have the same domains in  $x$ . We are also free to choose  $\psi_{max}$  to have the same value for the circular boundary solution and the perturbed solution. The common value of  $\psi_{max}$  can be normalized to 1.

One of the boundary conditions at the plasma boundary is:

$$\begin{aligned} \psi_v|_{r=1+r_{b1}(\theta)} = \psi_v^{(0)} + \psi_v^{(1)}|_{r=1+r_{b1}(\theta)} = 1 = \\ A_0^{(0)} + a_0^{(1)} + b_0^{(0)} r_{b1}(\theta) + \sum_{n=1}^{\infty} [(a_n^{(1)} + b_n^{(1)}) + 2a_n^{(0)} n r_{b1}(\theta)] \cos n\theta. \end{aligned} \quad (59)$$

To 1st order in  $\delta$  this gives:

$$a_0^{(1)} + \sum_{n=1}^{\infty} (a_n^{(1)} + b_n^{(1)}) \cos n\theta + (b_0^{(0)} + 2 \sum_{n=1}^{\infty} a_n^{(0)} n \cos n\theta) r_{b1}(\theta) = 0, \quad (60)$$

or

$$r_{b1}(\theta) = -\frac{a_0^{(1)} + \sum_{n=1}^{\infty} (a_n^{(1)} + b_n^{(1)}) \cos n\theta}{b_0^{(0)} + 2 \sum_{n=1}^{\infty} a_n^{(0)} n \cos n\theta}. \quad (61)$$

To 1st order in  $\delta$ , the radial derivative at the perturbed boundary is:

$$\begin{aligned} \frac{\partial \psi_v^{(1)}}{\partial r}|_{r=1+r_{b1}(\theta)} = b_0^{(1)} - b_0^{(0)} r_{b1}(\theta) \\ + \sum_{n=1}^{\infty} [(a_n^{(1)} - b_n^{(1)}) - 2a_n^{(0)} r_{b1}(\theta)] n \cos n\theta. \end{aligned} \quad (62)$$

We expand the relation (16) to 1st order:

$$2\left(\frac{\partial \psi_0^{(0)}}{\partial r}\right)_{\psi_0=1} \left(\frac{\partial \psi_0^{(1)}}{\partial r}\right)_{\psi_0=1} = 4\epsilon \bar{\beta}_p \left[ 4p_0(y) y r_{b1}(\theta) + 4 \int_{-1}^y p_1(x) dx \right], \quad (63)$$

where again  $y \equiv \cos \theta$ . It follows that

$$\left(\frac{\partial \psi_0^{(1)}}{\partial r}\right)_{\psi_0=1} = 2(\epsilon \bar{\beta}_p)^{1/2} \left[ \frac{p_0 y}{\sqrt{\int_{-1}^y p_0(x) dx}} r_{b1}(\theta) + \frac{\int_{-1}^y p_1(x) dx}{\sqrt{\int_{-1}^y p_0(x) dx}} \right] \quad (64)$$

The zero surface-current assumption connects (64) and (62) and gives:

$$a_0^{(1)} + b_0^{(1)} + \sum_{n=1}^{\infty} [(n+1)a_n^{(1)} - (n-1)b_n^{(1)}] \cos n\theta = \frac{p_0 y (\epsilon \bar{\beta}_p)^{1/2}}{\sqrt{\int_{-1}^y p_0(x) dx}} r_{b1}(\theta) + \frac{(\epsilon \bar{\beta}_p)^{1/2} \int_{-1}^y p_1(x) dx}{\sqrt{\int_{-1}^y p_0(x) dx}}, \quad (65)$$

where we have made use of equation(60).

We specify the perturbed boundary,  $r_{b1}(\theta) = \sum_{n=0}^{\infty} \alpha_n \cos n\theta$ . Eq. (60) then determines the perturbed vacuum field. Substituting the perturbed coefficients into Eq. (65), we get an equation that determines  $p_1(x)$  when we impose the constraints:

$$p_1(\pm 1) = 0 \quad (66)$$

When the magnetic field is vertical and uniform at infinity, (60) and (65) can be simplified into:

$$r_{b1}(\theta) = \sum_{n=0}^{\infty} \alpha_n \cos n\theta = \frac{a_0^{(1)} + a_1^{(1)} \cos \theta + \sum_{n=1}^{\infty} b_n^{(1)} \cos n\theta}{b_0^{(0)} (1 + \cos \theta)}, \quad (67)$$

and

$$a_0^{(1)} + b_0^{(1)} + 2a_1^{(1)} \cos \theta + \sum_{n=1}^{\infty} (1-n)b_n^{(1)} \cos n\theta = \frac{p_0 y (\epsilon \bar{\beta}_p)^{1/2}}{\sqrt{\int_{-1}^y p_0(x) dx}} r_{b1}(\theta) + \frac{(\epsilon \bar{\beta}_p)^{1/2} \int_{-1}^y p_1(x) dx}{\sqrt{\int_{-1}^y p_0(x) dx}}. \quad (68)$$

Fig. 2 shows the equilibrium solution for a perturbed plasma boundary with small ellipticity,

$$r_{b1}(\theta) = -0.03(1 - \cos 2\theta). \quad (69)$$

The detailed calculation for the perturbed vacuum field and the perturbed pressure is given in Appendix B.

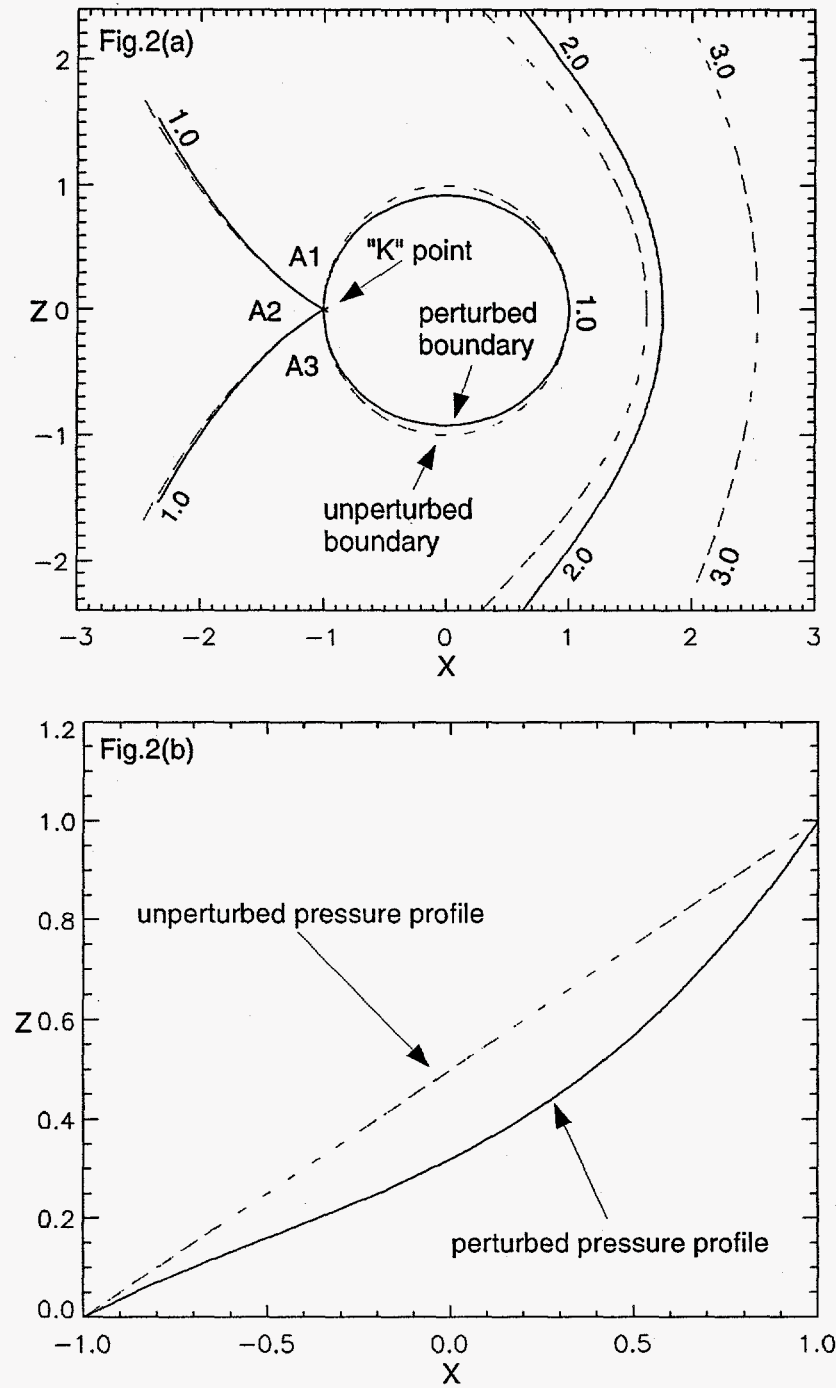


Figure 2: (a) Contour plot for vacuum solution, (b) Pressure profile. The dashed line is the unperturbed solution, and the solid line is the perturbed one.



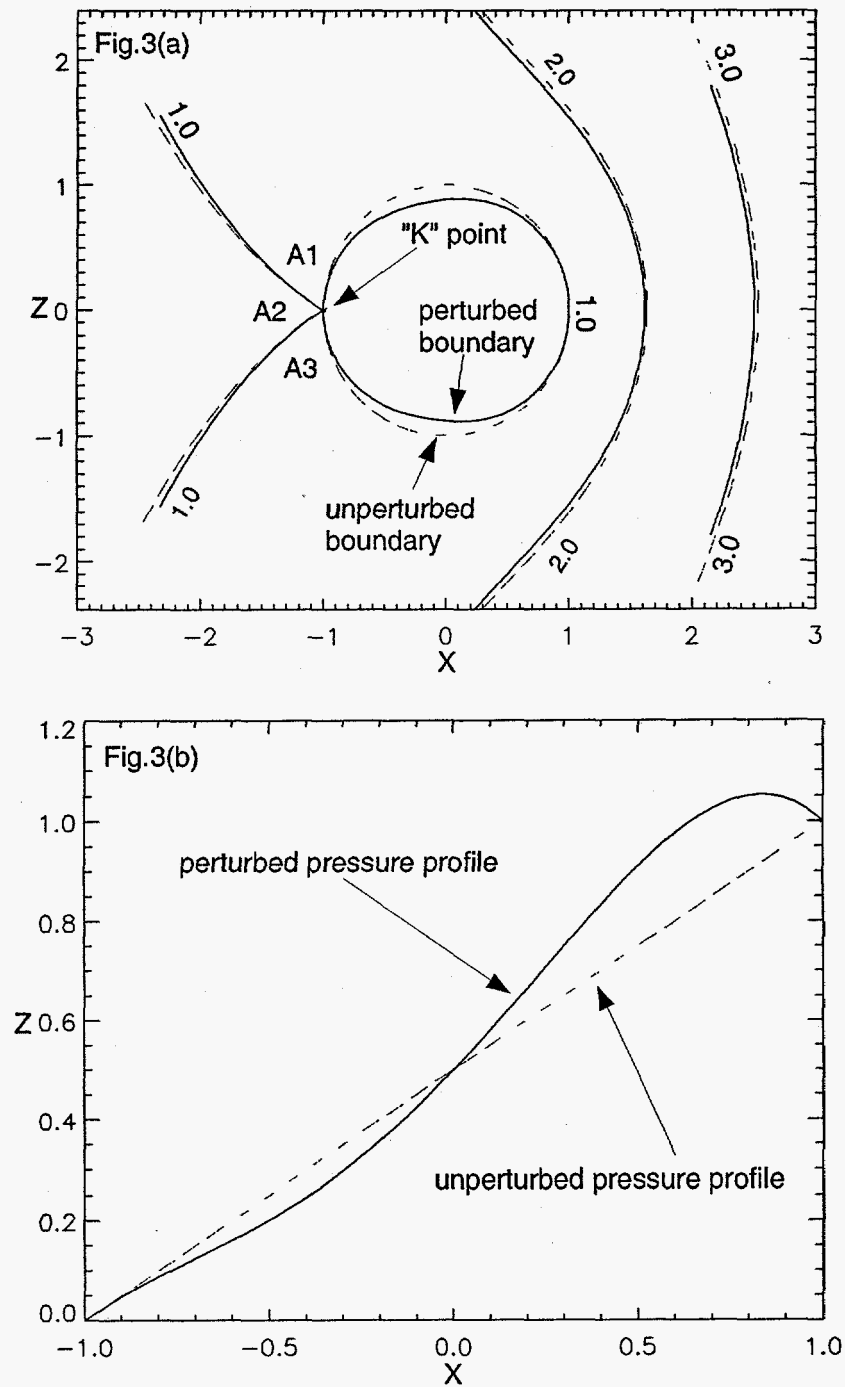


Figure 3: (a) Contour plot for vacuum solution, (b) Pressure profile. The dashed line is the unperturbed solution, and the solid line is the perturbed one.

Fig. 3 shows the equilibrium solution for a perturbed plasma boundary with small ellipticity and triangularity,

$$r_{b1}(\theta) = -0.05(1 - \cos 2\theta) + 0.015(\cos \theta - \cos 3\theta). \quad (70)$$

The detailed calculation is again given in Appendix B.

The perturbation does not alter the main topological features we found in the presence of a circular boundary. Even though the global picture of  $\psi_v$  changes after the perturbation, the K-shaped structure with three equal angles at the leftmost boundary is kept to first order of  $\delta$ .

Considering equation (58) and (60), we must have two relations between the  $a_n^{(1)}, b_n^{(1)}$ :

$$a_0^{(1)} + \sum_{n=1}^{\infty} (a_n^{(1)} + b_n^{(1)})(-1)^n = 0, \quad (71)$$

and

$$-\sum_{n=1}^{\infty} (a_n^{(1)} + b_n^{(1)})(-1)^n n^2 = 0. \quad (72)$$

From equation (65) and (58), we obtain another relation between the coefficients:

$$a_0^{(1)} + b_0^{(1)} + \sum_{n=1}^{\infty} [(n+1)a_n^{(1)} - (n-1)b_n^{(1)}](-1)^n = 0. \quad (73)$$

Physically, this means that to 1st order in  $\delta$  the poloidal field at the leftmost boundary in the mid-plane is zero. This conclusion is consistent with equation (17).

Using the relations (71), (72) and (73), we find that to first order in  $\delta$  all the first and second derivatives vanish at the leftmost boundary in the mid-plane. As in section 3.2, we find:

$$\frac{\partial^3 \psi_v^{(1)}}{\partial r \partial \theta^2} \Big|_{r=1, \theta=\pi} = -\frac{\partial^3 \psi_v^{(1)}}{\partial r^3} \Big|_{r=1, \theta=\pi}, \quad (74)$$

$$\frac{\partial^3 \psi_v^{(1)}}{\partial r^2 \partial \theta} \Big|_{r=1, \theta=\pi} = \frac{\partial^3 \psi_v^{(1)}}{\partial \theta^3} \Big|_{r=1, \theta=\pi} = 0. \quad (75)$$

Here we have taken the radial and poloidal derivatives of the Laplace equation for  $\psi_v^{(1)}$  with the conditions that all the second derivatives at the leftmost boundary in the mid-plane vanish.

Following the argument in section 3.2, we find that the topological structure for  $\psi_v = \psi_v^{(0)} + \psi_v^{(1)}$  is the same as that for the unperturbed  $\psi_v^{(0)}$  with a circular boundary. See Fig. 2 and Fig. 3 for the perturbed boundary and perturbed vacuum solution.

## 5 Discussion and Conclusions

For a fixed boundary equilibrium solution, such as that described in reference [3], we are free to independently specify the shape of the boundary as well as two profiles. We can, for example, specify  $p(\psi)$  plus one other profile such as  $q(\psi)$ , or  $G(\psi)$ , or  $x(\psi)$ . The fixed boundary equilibrium solution does not take into account the constraints arising from coupling to a vacuum field outside the plasma. The extension to a free-boundary solution requires the existence of an appropriate vacuum field that can support the given profiles and plasma shape. We need to be concerned about whether the vacuum field to which we couple is physically realizable with a reasonable set of external field coils.

Specification of the fixed boundary solution determines  $p(\psi_0(x))$ . For a circular boundary, this quantity is related to the external vacuum field through equation (30). The higher  $n$  Fourier components of the vacuum field decay rapidly away from the external field coils. It is not desirable to have the external field coils very close to the plasma, and in practice only a few low  $n$  values of the  $a_n$  will be non-negligible. Equation (30) then dictates the limited class of  $p(\psi_0(x))$  profiles that are in practice consistent with a circular plasma boundary. This is a strong constraint on the practically realizable high  $\epsilon\beta_p$  equilibrium solutions that emerges from our analysis.

In experiments, we impose the part of the vacuum field produced by the coils. The profiles in the plasma are determined by the ohmic current drive and by any supplementary current drive, and by the density and temperature profiles, which are in turn determined through transport processes. The equilibrium equations self-consistently determine the shape of the plasma boundary in the presence of these profiles and the imposed external field. The solutions obtained in this paper correspond to those profiles which yield a nearly circular boundary. For a given boundary shape, and a set of  $a_n$  determined by the external coils, the vacuum field is determined by equation (60). Equation (65) in turn gives the  $p(x)$  profile required to yield the specified boundary with the given external field. One profile in the plasma interior remains arbitrary. We find that at high  $\epsilon\beta_p$  the pressure profile plays a key role in determining the boundary shape, in contrast with the situation at low  $\beta$ , where the shape is only weakly affected by the pressure profile.

Matching to the external vacuum field enables us to examine the topology of the flux surfaces. Consistent with the picture of a separatrix moving in as  $\epsilon\beta_p$  is increased, the plasma is bounded by a separatrix in our high  $\epsilon\beta_p$  equilibrium solutions. As we raise  $\beta_I\bar{\beta}_p$  in an equilibrium with circular boundary, the aperture decreases as described by Eq. (42). This relation is a consequence of our assumption that there is no surface current at the plasma-

vacuum interface. If we allow a surface current to exist at the plasm-vacuum interface, it can prevent the separatrix from moving in as the pressure is increased. Even in the absence of a surface current, we can construct a flux conserving sequence of equilibria by controlling the current profile as  $p_{max}$  is raised to keep the  $q$  profile invariant. In that case, the current increases with  $p_{max}$  to keep  $\beta_I \bar{\beta}_p$  invariant, consistent with Eq. (42).

## Appendix A The Derivation of Equation (7)

We expand equation (3) order by order in the parameter  $\alpha$ . To the order  $\alpha^0$  we get:

$$G_0(\psi_0) = 0. \quad (76)$$

To the order  $\alpha^1, \alpha^2, \dots, \alpha^{m-1}$ :

$$G_1(\psi_0) = 0, G_2(\psi_0) = 0, \dots, G_{m-1}(\psi_0) = 0. \quad (77)$$

To the order  $\alpha^m$ :

$$p'(\psi_0) + G_m(\psi_0) = 0. \quad (78)$$

To the order of  $\alpha^{m+1}, \alpha^{m+2}, \dots, \alpha^{m+n-1}$ :

$$G_{m+1}(\psi_0) = 0, G_{m+2}(\psi_0) = 0, \dots, G_{m+n-1}(\psi_0) = 0. \quad (79)$$

To the order of  $\alpha^{m+n}$

$$2xp'(\psi_0) + G_{m+n}(\psi_0) = 0. \quad (80)$$

The last equation is equation (7).

## Appendix B Calculation of the First Order Solution with a Perturbed Boundary

We normalize  $p_0(x), p_1(x)$  by  $(\epsilon \bar{\beta}_p)^{-1} (b_0^{(0)})^2$  and  $a_0^{(1)}, a_1^{(1)}$  and  $b_n^{(1)}$  by  $b_0^{(0)}$ , then substitute equation (67) into (68), multiply both sides of the equation by  $1 + \cos(\theta)$ , and equate the corresponding Fourier coefficients. This procedure leads us to the following set of equations:

$$2f_0 = a_0^{(1)} + 1.5a_1^{(1)} + b_0^{(1)} + 0.5b_1^{(1)},$$

$$\begin{aligned}
2f_1 &= 2a_0^{(1)} + 2a_1^{(1)} + b_0^{(1)}, \\
2f_2 &= 1.5a_1^{(1)} + 0.5b_1^{(1)} - b_2^{(1)} - 0.5b_3^{(1)}, \\
2f_3 &= -2b_3^{(1)} - b_4^{(1)}, \\
&\dots \\
2f_m &= -\frac{m-3}{2}b_{m-1}^{(1)} - (m-1)b_m^{(1)} - \frac{m-1}{2}b_{m+1}^{(1)} \quad (m > 2), \quad (81)
\end{aligned}$$

where the  $f_n$  are the Fourier component of  $\int_{-1}^{\cos(\theta)} p_1(x) dx$ ,

$$\int_{-1}^{\cos(\theta)} p_1(x) dx = \sum_{n=0}^{\infty} f_n \cos n\theta.$$

The quantity  $p_1(x)$  is given by

$$p_1(x) = \sum_{n=0}^{\infty} f_n \frac{dT_n(x)}{dx} = \sum_{n=0}^{\infty} f_n n U_{n-1}(x), \quad (82)$$

where  $T_n(x)$  and  $U_n(x)$  are Chebyshev polynomials of the first kind and second kind.

Equation (67) gives:

$$\begin{aligned}
a_0^{(1)} &= -\alpha_0 - 0.5\alpha_1, \\
a_1^{(1)} + b_1^{(1)} &= -\alpha_0 - \alpha_1 - 0.5\alpha_2, \\
b_2^{(1)} &= -0.5\alpha_1 - \alpha_2 - 0.5\alpha_3, \\
&\dots \\
b_n^{(1)} &= -0.5\alpha_{n-1} - \alpha_n - 0.5\alpha_{n+1} \quad (n > 1).
\end{aligned}$$

When  $\alpha_n$  is specified,  $a_0^{(1)}$ ,  $a_1^{(1)}$ ,  $b_n^{(1)}$ , and  $p_1(x)$  can be determined from the above equations together with constraint  $p_1(\pm 1) = 0$ . The constraint is needed because the above equations have two undetermined degrees of freedom.  $b_0^{(1)}$  is determined through equation (73).

For example, when  $r_{b1}(\theta) = -0.03(1 - \cos 2\theta)$ , we obtain  $a_0^{(1)} = 0.03$ ,  $a_1^{(1)} = -0.075$ ,  $a_n^{(1)} = 0$  ( $n > 1$ ),  $b_0^{(1)} = -0.18$ ,  $b_1^{(1)} = 0.09$ ,  $b_2^{(1)} = -0.03$ ,  $b_3^{(1)} = -0.015$ ,  $b_n^{(1)} = 0$  ( $n > 3$ ), and  $p_1(x) = -0.18 - 0.12x + 0.18x^2 + 0.12x^3$ . The solution is shown in Fig. 2.

When  $r_{b1}(\theta) = -0.05(1 - \cos 2\theta) + 0.015(\cos \theta - \cos 3\theta)$ , we obtain  $a_0^{(1)} = 0.0425$ ,  $a_1^{(1)} = 0.01$ ,  $a_n^{(1)} = 0$  ( $n > 1$ ),  $b_0^{(1)} = -0.03$ ,  $b_1^{(1)} = 0$ ,  $b_2^{(1)} = -0.05$ ,  $b_3^{(1)} = -0.01$ ,  $b_4^{(1)} = 0.0075$ ,  $b_n^{(1)} = 0$  ( $n > 4$ ), and  $p_1(x) = 0.28x + 0.3x^2 - 0.28x^3 - 0.3x^4$ . The solution is shown in Fig. 3.

## References

- [1] S.A. Sabbagh, R.A. Gross, M.E. Mauel, G.A. Navratil, M.G. Bell, R. Bell, M. Bitter, N.L. Bretz, R.V. Budny, C.E. Bush, M.S. Chance, P.C. Efthimion, E.D. Fredrickson, R. Hatcher, R.J. Hawryluk, S.P. Hirshman, A.C. Janos, S.C. Jardin, D.L. Jassby, J. Manickam, D.C. McCune, K.M. McGuire, S.S. Medley, D. Mueller, Y. Nagayama, D.K. Owens, M. Okabayashi, H.K. Park, A.T. Ramsey, B.C. Stratton, E.J. Synakowski, G. Taylor, R.M. Wieland, M.C. Zarnstorff, J. Kesner, E.S. Marmor, and J.L. Terry, *Phys. Fluids B* **3**, 2277 (1991).
- [2] M.E. Mauel, G.A. Navratil, S.A. Sabbagh, M.G. Bell, R.V. Budny, E.D. Fredrickson, R.J. Hawryluk, A.C. Janos, D.W. Johnson, D.C. McCune, K.M. McGuire, S.S. Medley, D. Mueller, D.K. Owens, H.K. Park, A.T. Ramsey, B.C. Stratton, E.J. Synakowski, G. Taylor, R.M. Wieland, M.C. Zarnstorff, J. Kesner, E.S. Marmor, and J.L. Terry, *Nucl. Fusion* **32**, 1468 (1992).
- [3] S.C. Cowley, P.K. Kaw, R.S. Kelly, and R.M. Kulsrud, *Phys. Fluids B* **3**, 2066 (1991)
- [4] J.P. Freidberg, *Ideal Magnetohydrodynamics* (Plenum, New York, 1987), pp. 132-145.